Optical Asymmetric Modulation for VLC Systems

(Invited Paper)

Hanaa Marshoud[1], Sami Muhaidat[1], Paschalis C. Sofotasios[1,2], Muhammad Imran[3], Bayan S. Sharif[1], and George K. Karagiannidis[4]

[1]Department of Electrical and Computer Engineering, Khalifa University of Science and Technology, 127788, Abu Dhabi, United Arab Emirates
e-mail: {hanaa.marshoud; sami.muhaidat; paschalis.sofotasios; bayan.sharif}@kustar.ac.ae
[2]Department of Electronics and Communications Engineering, Tampere University of Technology, FI-33101, Tampere, Finland, e-mail: paschalis.sofotasios@tut.fi
[3]School of Engineering, University of Glasgow, G12 8QQ, Glasgow, Scotland, United Kingdom, e-mail: Muhammad.Imran@glasgow.ac.uk
[4]Department of Electrical and Computer Engineering, Aristotle University of Thessaloniki, GR-51124, Thessaloniki, Greece, e-mail: geokarag@auth.gr

***Abstract*—The explosive growth of connected devices and the increasing number of broadband users have led to an unprecedented growth in traffic demand. To this effect, the next generation wireless systems are envisioned to meet this growth and offer a potential data rate of 10 Gbps or more. In this context, an attractive solution to the current spectrum crunch issue is to exploit the visible light spectrum for the realization of high-speed commutation systems. However, this requires solutions to certain challenges relating to visible light communications (VLC), such as the stringent requirements of VLC-based intensity modulation and direct detection (IM/DD), which require signals to be real and unipolar. The present work proposes a novel power-domain multiplexing based optical asymmetric modulation (OAM) scheme for indoor VLC systems, which is particularly adapted to transmit high-order modulation signals using linear real and unipolar constellations that fit into the restrictions of IM/DD systems. It is shown that the proposed scheme provides improved system performance that outperforms alternative modulation schemes, at no extra complexity.**

I. Introduction

The evolving next generation networks are envisioned to face an inevitable surge in wireless data traffic, because of the looming increase in the number of interconnected devices that constitute a core component of the Internet of Things (IoT). As a result, the information and communication technology (ICT) industry seeks ground-breaking solutions to enhance the capacity and coverage of wireless communication systems. In this regard, the key objectives of future networks include: 1) improving the spectral efficiency of the radio frequency (RF) spectrum by adopting advanced modulation and transmission techniques; 2) enhancing the mobile networks coverage by the deployment of small cells; and 3) optimizing the spectrum usage by combining licensed and unlicensed frequency bands.

Motivated by the advancements in light-emitting-diodes (LEDs), visible light communications (VLC) has recently emerged as a potential enabler for next generation networks [1]. VLC is a small-cell technology that exploits the unregulated visible light spectrum for short-range data transmission using intensity modulation and direct detection (IM/DD). To this end, the LED driving electrical current is varied according to the transmitted symbols, whilst the respective variations of the radiated optical power are not visible to the human eye, due to the relatively high switching rate of the LEDs. At the receiver terminal, a photo detector (PD) is used to translate the fluctuations in the received beams into current that is used for data recovery [2], [3]. In this context, the interest in VLC technology is based on the wide deployment of LEDs in residential and public buildings as well as street and traffic lights, which means that the infrastructure for VLC already exists and can be exploited after minimal hardware adjustments. Moreover, VLC can contribute to reducing the energy consumptions in cellular base stations by offloading a part of the data traffic. This is a critical concern for 5G networks because the ICT sector already impacts substantially the global carbon footprint. Also, the fact that VLC transmissions do not interfere with RF communications offers high degrees of spatial reuse and immunity to electromagnetic interference.

The achievable data rates in VLC systems are limited by the available modulation bandwidth, which is primarily constrained by the response time of the LED devices. Moreover, the nature of IM/DD restricts VLC transmissions to real and positive constellations, which renders the implementation of high order complex modulation schemes unviable [4]. As a result, the development of new transmission schemes and network infrastructure solutions to enable high data-rate VLC systems has attracted enormous attention in the recent years. To this end, several multiple-input-multiple-output (MIMO) configurations have been recently proposed to enhance the spectral efficiency of VLC systems [5]–[7], such as spatial multiplexing (SMP), where independent data streams are emitted simultaneously from different transmitting LEDs to multiple receiving PDs. In SMP, the underlying MIMO

978-1-5386-6355-4/18/$31.00 ©2018 IEEE

channel is converted into a set of parallel independent subchannels by utilizing precoding and/or equalization [8]–[12]. Zeng et al. [13] demonstrated that SMP improves the spectral efficiency of indoor VLC systems by exploiting multiplexing gains. In order to achieve these gains, sufficiently low correlation between the MIMO subchannels is required. However, the symmetric nature of the VLC channel results in highly correlated links, particularly, in scenarios where multipath reflections are negligible [14]. Potential solutions to reduce the high channel correlation between the subchannels in VLC include power imbalance and link blockage [15]. However, such techniques may lead to significant degradation in the corresponding energy efficiency of the system.

Spatial modulation (SM) has been also adopted in VLC systems as it is another MIMO technique that uses the index of the transmitting LED as an additional source of information to improve the overall system spectral efficiency [16], [17]. Recently, space shift keying (SSK) modulation has been proposed as a variant of SM in which the indices of the transmitting LEDs constitute constellation symbols [18]. In particular, a single transmitting LED is activated at any symbol duration, such that the spatial position of the transmitting LED determines the transmitted symbol. Based on this, a spatial constellation of N_t possible symbols is realized, where N_t denotes the total number of LEDs. The spectral efficiency of SSK was further improved by proposing generalized SSK (GSSK) [19]–[21], in which multiple transmitting LEDs are activated at each symbol duration, yielding 2^{N_t} possible spatial symbols. It is worth noting that spatial-based modulation techniques require independent spatial links, which is impractical in VLC systems due to the symmetric nature of VLC channels.

The present contribution proposes a novel optical asymmetric modulation (OAM) scheme that is capable of enabling high-rate transmission in indoor VLC systems. In OAM, an $M-$ary transmission is achieved by representing each symbol by a unique sum of trigonometric functions of predefined angles. The main characteristic of the proposed scheme is its low hardware complexity, where a high-order modulation is realized using a single transmitting LED and a single receiving PD. Furthermore, the proposed scheme is robust to the high correlation between the VLC subchannels, which is a common impediment in MIMO-based solutions. As a result, OAM can be rather useful in the effective deployment of VLC systems.

II. System and Channel Model

A generic indoor VLC system is considered where the proposed OAM is realized by means of a single transmitting LED and a single receiving PD. We also consider a line-of-sight (LOS) indoor downlink VLC transmission, as shown in Fig.1, where multipath delays resulting from reflections and diffuse refractions are not considered because they are typically negligible in indoor VLC scenarios [22]. The VLC channel gain between the LED and the PD is expressed as

$$h = \begin{cases} \frac{A}{d^2} R_o(\varphi) T_s(\phi) g(\phi) \cos(\phi), & 0 \le \phi \le \phi_c \\ 0, & \phi > \phi_c \end{cases} \quad (1)$$

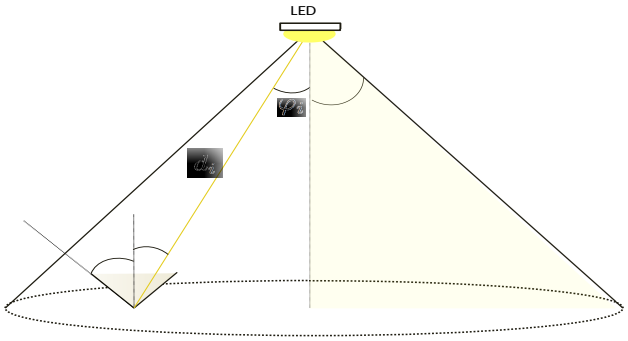

Fig. 1: VLC channel model.

where A denotes the receiving PD area, d is the distance between the LED and the PD, φ is the angle of emergence with respect to the transmitter axis, ϕ is the angle of incidence with respect to the receiver axis, ϕ_c is the field of view (FOV) of the PD, $T_s(\phi)$ is the gain of the optical filter and $g(\phi)$ is the gain of the optical concentrator, which is given by

$$g(\phi) = \begin{cases} \frac{n^2}{\sin^2(\phi_c)}, & 0 \le \phi \le \phi_c \\ 0, & \phi > \phi_c \end{cases} \quad (2)$$

where n denotes the corresponding refractive index. Moreover, $R_o(\varphi)$ in (1) is the Lambertian radiant intensity of the transmitting LEDs, which can be expressed as $R_o(\varphi) = (m+1)\cos^m(\varphi)/(2\pi)$, where $m = -\ln(2)/\ln(\cos(\varphi_{1/2}))$ is the order of Lambertian emission, with $\varphi_{1/2}$ denoting the transmitter semi-angle at half power. Moreover, the noise at the receiving terminal is drawn from a circularly-symmetric Gaussian distribution of zero mean and variance $\sigma_n^2 = \sigma_{\rm sh}^2 + \sigma_{\rm th}^2$, where $\sigma_{\rm sh}^2$ and $\sigma_{\rm th}^2$ are the variances of the shot noise and thermal noise, respectively [23]. The shot noise in optical wireless channels is generated by the high rate physical photo-electronic conversion process, and its variance is expressed as

$$\sigma_{\rm sh}^2 = 2qB\left(\gamma h P_x + I_{\rm bg} I_2\right) \quad (3)$$

where q is the electronic charge, γ is the detector responsivity, P_x is the signal power, B is the corresponding bandwidth, $I_{\rm bg}$ is background current, and I_2 is the noise bandwidth factor. Furthermore, the thermal noise is generated within the transimpedance receiver circuitry, and its variance is given by

$$\sigma_{\rm th}^2 = \frac{8\pi K T_k}{G}\eta A I_2 B^2 + \frac{16\pi^2 K T_k \Gamma}{g_m}\eta^2 A^2 I_3 B^3 \quad (4)$$

where K is Boltzmann's constant, T_k is the absolute temperature, G is the open-loop voltage gain, A is the PD area, η is the fixed capacitance of the PD per unit area, Γ is the field-effect transistor (FET) channel noise factor, g_m is the FET transconductance, and I_3 = 0.0868 [23].

III. Optical Asymmetric Modulation (OAM)

In this section, we present a novel power-domain multiplexing based modulation scheme that can be used to trans-

mit high-order modulation signals over VLC channels. The proposed OAM scheme generates real unipolar signals that fit into the restrictions of IM/DD. Specifically, an $M-$ary modulation order can be realized by representing each of the M symbols in the constellation diagram as the summation of the cosine and sine functions of predefined angles. The resultant signals are then superimposed in the power domain and sent simultaneously, i.e., using the same bandwidth and time resources. The linear constellation vector in OAM can be represented as follows:

$$S_M = [s(\theta_1) \quad s(\theta_2) \quad s(\theta_3) \quad ... \quad s(\theta_{M/4})]^T \tag{5}$$

where M is the modulation order, and

$$\begin{aligned} s(\theta_i) =&[\cos(\theta_i) + \sin(\theta_i) \quad \cos(\theta_i) - \sin(\theta_i) \\ &- \cos(\theta_i) + \sin(\theta_i) \quad - \cos(\theta_i) - \sin(\theta_i)]^T. \end{aligned} \tag{6}$$

In what follows, we provide two specific examples for 4-ary and 8-ary modulations.

Example 1: Considering 4-ary OAM, with angle θ_1, the four intensity modulation levels are determined as follows

$$s_M = \begin{cases} \cos(\theta_1) + \sin(\theta_1), & m = 1 \\ \cos(\theta_1) - \sin(\theta_1), & m = 2 \\ -\cos(\theta_1) + \sin(\theta_1), & m = 3 \\ -\cos(\theta_1) - \sin(\theta_1), & m = 4 \end{cases} \tag{7}$$

Note that the formed constellation constitutes of real symbols which, after adding a DC bias, can be directly transmitted in IM/DD based VLC systems. The proposed constellation design can be extended to higher order modulations by adding new angles, where the bits after the two least significant bits in each symbol determine the angle to be used. Consequently, 2^{N-2} different angles are required to generate the M constellation levels, where $N = \log_2(M)$ is the number of bits per symbol.

Example 2: Considering 8-ary OAM, the 8 constellation levels are given as

$$s_M = \begin{cases} \cos(\theta_1) + \sin(\theta_1), & m = 1 \\ \cos(\theta_1) - \sin(\theta_1), & m = 2 \\ -\cos(\theta_1) + \sin(\theta_1), & m = 3 \\ -\cos(\theta_1) - \sin(\theta_1), & m = 4 \\ \cos(\theta_2) + \sin(\theta_2), & m = 5 \\ \cos(\theta_2) - \sin(\theta_2), & m = 6 \\ -\cos(\theta_2) + \sin(\theta_2), & m = 7 \\ -\cos(\theta_2) - \sin(\theta_2), & m = 8 \end{cases} \tag{8}$$

where the first four levels are generated using θ_1 and the rest using θ_2. Based on this, an M-ary transmitted signal in OAM can be written as

$$x = \frac{1}{2\delta} P_{\text{LED}} \, (s_m + \delta) \tag{9}$$

where P_{LED} is the LED peak power and δ is a DC bias added to ensure positivity. It is worth noting that the value of δ is chosen to meet the highest value of the generated symbols. Likewise, the signal power in (9) is normalized by 2δ prior to transmission in order to ensure that the maximum transmit power does not exceed the LED peak power.

At the receiving terminal, the received signal is given by $r = \gamma h x + n$, where γ denotes the detector responsivity, h is the VLC channel gain given by (1), and n denotes zero-mean additive white Gaussian noise (AWGN) with variance σ_n^2. After removing the DC bias, the estimated symbol $\hat{s}_m$ is obtained based on the Euclidean distance receiver, namely

$$\hat{s}_m = \arg\min_{s_m} \left| r - \frac{1}{2\delta} \gamma P_{\text{LED}} h s_m \right|^2. \tag{10}$$

IV. Comparison with SMP and GSSK

In this section, we compare the proposed OAM scheme with the state-of-the-art modulation schemes targeting high-rate transmissions in VLC systems. Specifically, we compare OAM with OOK-based SMP and GSSK modulation. In SMP, independent data streams are simultaneously transmitted from N_t different LEDs, providing an enhanced spectral efficiency of N_t bit/s/Hz [15]. Transmit precoding using channel inversion [9] is performed prior to signal transmission in order to establish parallel MIMO channels for SMP. Moreover, we consider optical spatial modulation by means of GSSK [16]. Different from conventional SSK [18], in which only one transmitter is active at a time while the others are idle, GSSK employs multiple simultaneous transmissions from the spatially separated LEDs, where each LED transmits an OOK signal depending on the intended symbol. Each constellation symbol is represented by a specific selection of the active and idle LEDs, thus, an $M-$ary modulation can be realized using $N_t = \log_2(M)$ transmitters [19]–[21]. Table I depicts the average transmitted power and hardware requirements for the different modulation schemes for a fixed spectral efficiency of $\log_2(M)$ bit/s/Hz.

V. Numerical Results and Discussions

In this section, we quantify the performance of the proposed OAM scheme for different scenarios, adopting the system and channel models presented in Section II. Extensive Monte Carlo simulations are provided to corroborate the analytic results and to provide detailed performance comparisons among the competing schemes presented in Section IV. We consider one transmitting LED to transmit 4-ary, 8-ary and 16-ary OAM signals. For SMP and GSSK schemes, we employ 2, 3 and 4 LEDs to transmit 4-ary, 8-ary and 16-ary modulations, respectively. For a fair comparison, the average transmitting power is unified for all the different schemes. The LEDs are located within a 4.0m $\times$ 4.0m $\times$ 3.0m room at a height of $z = 3$m and are oriented downwards to point straight down from the ceiling; the receiving PDs are placed at a height of $z = 0.75$m and are oriented upwards towards the ceiling. The locations of the transmitting LEDs and receiving PDs are shown in Table II, where OAM uses only LED1 and PD1, GSSK uses all LEDs and PD1 and SMP uses all LEDs and

TABLE I: Comparison of Different Modulation Schemes.

Modulation Scheme	Average Power (P_{avg})	Number of LEDs (N_t)	Number of PDs (N_r)
SMP	$\log_2(M)\frac{P_t}{2}$	$\log_2(M)$	$\log_2(M)$
GSSK	$\log_2(M)\frac{P_t}{2}$	$\log_2(M)$	1
OAM	$\frac{P_t}{2}$	1	1

all PDs depending on the modulation order. The remaining system parameters are depicted in Table III.

TABLE II: Locations of Transmitting LEDs.

LED	Coordinates	PD	Coordinates
LED1	(2.2,2.2,3)	PD1	(1.9,1.8,0.75)
LED2	(1.8,2.2,3)	PD2	(2,1.9,0.75)
LED3	(1.8,1.8,3)	PD3	(2.2,2,0.75)
LED4	(2.2,1.8,3)	PD4	(2.3,2.1,0.75)

We compare the error performance of the proposed OAM scheme with the competing schemes presented in Section IV. Fig. 2 illustrates the SER performance of OAM versus SMP as a function of the signal to noise ratio (SNR), where the latter employs $\log_2(M)$ transmitting LEDs and $\log_2(M)$ receiving PDs. It is clear from Fig. 2 that that OAM outperforms SMP for different modulation orders. For example, for 4-ary modulation, OAM provides an enhancement of about 20dB compared to SMP at SER of 10^{-3}. This is mainly

TABLE III: Simulation Parameters.

Description	Notation	Value
LED power	P_{LED}	0.25 W
Transmitter semi-angle	φ_i	30 deg
FOV of the PDs	ϕ_{c_i}	15 deg
Physical area of PD	A_i	1.0 cm^2
PD responsivity	γ	$1A/W$
Refractive index of PD lens	n	1.5
Gain of optical filter	$T_s(\phi_{li})$	1.0

due to the noise enhancement in SMP caused by the channel inversion precoding performed prior to signal transmission, which is dependent on the degree of correlation between the MIMO subchannels. It is worth noting that the performance of SMP can be improved by increasing the spacing between the receiving PDs; however, this may not be practical due to size limitations. It is also emphasized that the proposed OAM outperforms SMP, while maintaining lower hardware complexity compared to SMP-based systems.

Fig. 3 compares the error performance of OAM with GSSK as a function of the SNR. It is observed that OAM provides performance gain compared to GSSK despite the fact that GSSK employs multiple transmitting LEDs. For 8-ary modulation, OAM outperforms GSSK by about 10dB at SER of 10^{-3}. This is because the level distinction in GSSK is based on the channel gains associated with the different symbols. It is also noted that GSSK requires the channel gains to be dissimilar for better performance; however, such a requirement may not be practical due to the highly symmetrical nature of the indoor

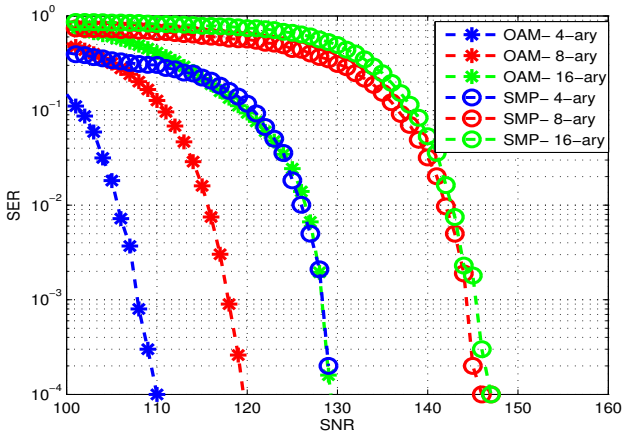

Fig. 2: SER vs SNR performance of OAM vs SMP.

VLC channels. In fact, certain receiver locations can exhibit very similar, and even identical, channel gains which leads to detrimental performance degradation of GSSK.

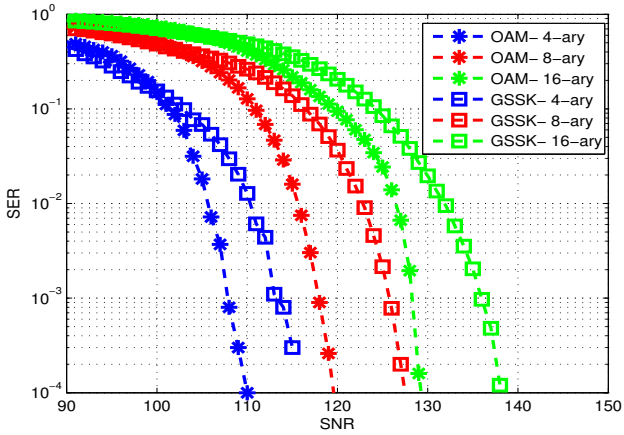

Fig. 3: SER vs SNR performance of OAM vs GSSK.

In the following, we evaluate the performance of the proposed OAP scheme assuming user mobility where the user locations are randomly generated within a circle of radius 2m. Fig. 4 shows the SER performance across the simulation area for a 4-ary transmission using OAM, SMP and GSSK, for an SNR of 120dB. For these results, a single transmitting LED is used for OAM, while SMP and GSSK use two transmitting LEDs that are located in the center of the room with a spacing of 0.1m. It is noted that SMP needs a strong channel gain to provide acceptable performance, and it experiences significant

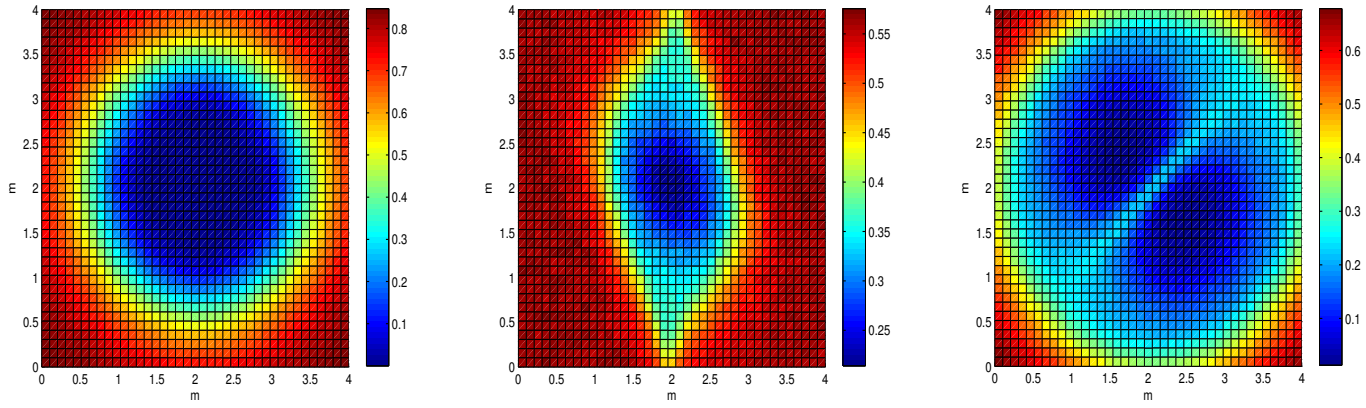

(a) (b) (c)

Fig. 4: SER across the simulation area for $4-$ary transmission at SNR = 120 dB using: (a) OAM; (b) SMP; and (c) GSSK.

performance degradation as the user moves away from the proximity of the LEDs. The SER performance of GSSK exhibits a severe degradation in the diagonal of the room, since at these locations the user observes highly correlated channel gains from the two transmitters due to the symmetric nature of the VLC channel. It is noted here that the performance non-uniformity for GSSK becomes more severe for higher modulation orders, as a higher number of transmitters will be used to convey the desired symbols. As demonstrated, the proposed OAM provides the best performance compared to other schemes while maintaining low hardware complexity.

VI. Conclusion

We proposed a novel optical asymmetric modulation (OAM) scheme to facilitate the efficient transmission of high order modulation signals over VLC channels. The error performance of the proposed scheme was compared with SMP and GSSK schemes for different modulation orders. It was shown that, although OAM uses a single LED and a single PD, it outperforms MIMO-based SMP and GSSK due to its robustness to the high correlation inherit in the indoor VLC subchannels. Furthermore, for the scenario involving user mobility, OAM was shown to provide the best uniform performance as SMP and GSSK exhibited severe performance non-uniformity.

References

[1] H. Burchardt, N. Serafimovski, D. Tsonev, S. Videv, and H. Haas, "VLC: Beyond point-to-point communication," *IEEE Commun. Mag*, vol. 52, no. 7, pp. 98–105, July 2014.

[2] S. Dimitrov, and H. Haas, *Principles of LED Light Communications: Towards Networked Li-Fi*. Cambridge University Press, 2015.

[3] J. Grubor, S. Randel, K.-D. Langer, and J. Walewski, "Broadband information broadcasting using LED-based interior lighting," *J. Lightw. Technol.*, vol. 26, no. 24, pp. 3883–3892, Dec. 2008.

[4] D. Karunatilaka, F. Zafar, V. Kalavally, and R. Parthiban, "LED based indoor visible light communications: State of the art," *Commun. Surveys Tuts.*, vol. 17, no. 3, pp. 1649–1678, Aug. 2015.

[5] S. Navidpour, M. Uysal, and M. Kavehrad, "BER performance of free-space optical transmission with spatial diversity," *IEEE Trans. Wireless Commun.*, vol. 6, no. 8, pp. 2813–2819, Aug. 2007.

[6] Y.-J. Zhu, W.-F. Liang, J.-K. Zhang, and Y.-Y. Zhang, "Space-collaborative constellation designs for MIMO indoor visible light communications," *IEEE Photon. Technol. Lett.*, vol. 27, no. 15, pp. 1667–1670, Aug. 2015.

[7] A. Nuwanpriya, S. Ho, and C. Chen, "Indoor MIMO visible light communications: Novel angle diversity receivers for mobile users," *IEEE J. Sel. Areas Commun*, vol. 33, no. 9, pp. 1780–1792, Sep. 2015.

[8] Y. Hong, J. Chen, Z. Wang, and C. Yu, "Performance of a precoding MIMO system for decentralized multiuser indoor visible light communications," *IEEE Photon. J.*, vol. 5, no. 4, pp. 7 800 211, Aug 2013.

[9] H. Marshoud, D. Dawoud, V. Kapinas, G. K. Karagiannidis, S. Muhaidat, and B. Sharif, "MU-MIMO precoding for VLC with imperfect CSI," in *Proc. 4th IWOW '15*, Sep. 2015, pp. 93–97.

[10] K. Ying, H. Qian, R. Baxley, and S. Yao, "Joint optimization of precoder and equalizer in MIMO VLC systems," *IEEE J. Sel. Areas Commun*, vol. 33, no. 9, pp. 1949–1958, Sep. 2015.

[11] H. Marshoud, P. C. Sofotasios, S. Muhaidat, B. S. Sharif, and G. K. Karagiannidis, "Optical Adaptive Precoding for Visible Light Communications," *IEEE Access*, To appear.

[12] H. Shen, Y. Deng, W. Xu, and C. Zhao, "Rate maximization for downlink multiuser visible light communications," *IEEE Access*, vol. 4, pp. 6567–6573, 2016.

[13] L. Zeng, D. O'brien, H. Minh, G. Faulkner, K. Lee, D. Jung, Y. Oh, and E. T. Won, "High data rate multiple input multiple output (MIMO) optical wireless communications using white LED lighting," *IEEE J. Sel. Areas Commun*, vol. 27, no. 9, pp. 1654–1662, Dec. 2009.

[14] P. F. Mmbaga, J. Thompson, and H. Haas, "Performance analysis of indoor diffuse VLC MIMO channels using angular diversity detectors," *J. Lightw. Technol.*, vol. 34, no. 4, pp. 1254–1266, Feb. 2016.

[15] T. Fath, and H. Haas, "Performance comparison of mimo techniques for optical wireless communications in indoor environments," *IEEE Trans. Commun.*, vol. 61, no. 2, pp. 733–742, Feb. 2013.

[16] R. Mesleh, H. Elgala, and H. Haas, "Optical spatial modulation," *IEEE J. Opt. Commun. Netw.*, vol. 3, no. 3, pp. 234–244, Mar. 2011.

[17] K. Cai, and M. Jiang, "SM/SPPM aided multiuser precoded visible light communication systems," *IEEE Photon. J.*, vol. 8, no. 2, pp. 1–9, Apr. 2016.

[18] S. Videv, and H. Haas, "Practical space shift keying VLC system," in *Proc. IEEE WCNC '14*, Apr. 2014, pp. 405–409.

[19] W. O. Popoola, E. Poves, and H. Haas, "Error performance of generalised space shift keying for indoor visible light communications," *IEEE Trans. Commun.*, vol. 61, no. 5, pp. 1968–1976, May 2013.

[20] W. O. Popoola, and H. Haas, "Demonstration of the merit and limitation of generalised space shift keying for indoor visible light communications," *J. Lightw. Technol.*, vol. 32, no. 10, pp. 1960–1965, May 2014.

[21] Y. Sun, D. K. Borah, and E. Curry, "Optimal symbol set selection in GSSK visible light wireless communication systems," *IEEE Photon. Technol. Lett.*, vol. 28, no. 3, pp. 303–306, Feb. 2016.

[22] I. Moreno, and C.-C. Sun, "Modeling the radiation pattern of LEDs," *Opt. Express*, vol. 16, no. 3, pp. 1808–1819, Feb. 2008.

[23] T. Komine, and M. Nakagawa, "Fundamental analysis for visible-light communication system using LED lights," *IEEE Trans. Consum. Electron.*, vol. 50, no. 1, pp. 100–107, Feb. 2004.